APPARATUS FOR MECHANICAL TESTING OF SOFT CRYSTALS AT HIGH PRESSURE

S. H. Gelles

Technical Report - 164

Technical Report Number 164

February 1968

Apparatus for Mechanical Testing of Soft Crystals at High Pressure

S. H. Gelles

Ledgemont Laboratory

Kennecott Copper Corporation

Lexington, Massachusetts 02173

Technical Report Number 164

February 1968

Apparatus for Mechanical Testing of Soft Crystals at High Pressure

S. H. Gelles

Abstract

Apparatus which has sufficient sensitivity for the tensile testing of soft single crystals at pressure levels to approximately 30 kbars is described. This equipment makes use of a tensile yoke and a load cell based on a linear variable differential transformer within the high pressure fluid. Strain is measured externally by monitoring the movement of the loading piston with a linear variable differential transformer and the load-displacement relationship is displayed on an X-Y recorder. Discussion of the calibration procedure and performance of the apparatus is included.

Ledgemont Laboratory

Kennecott Copper Corporation

Lexington, Massachusetts 02173

Apparatus for Mechanical Testing of Soft Crystals at High Pressure

S. H. Gelles

Introduction

In order to measure the initial flow stress of soft single crystals in a high hydrostatic pressure environment, it was necessary to develop apparatus for applying tensile loads to the sample and for measuring the load-extension relationship and thereby the resolved shear stress - shear strain relationship. Since only small changes were expected in the critical resolved shear stress with pressure, it was considered essential to make measurements at the highest possible pressure. The pressure limitation is due to the solidification of the pressure transmitting medium. It was felt that 50-50% mixture of n- and i- pentane (a common high pressure medium because of its high solidification pressure) could be used to approximately 30 kbars without encountering non-hydrostaticity effects[1,2] i.e., the presence of significant shear stresses in the fluid since these would lead to undesirable deformation of the samples. The zinc single crystals that were to be tested have critical resolved shear stresses at atmospheric pressure of as little as $20/gm/mm^2$

corresponding to an applied load of 280 gm on a crystal having an orientation, $\phi_o = 45^o$, $\lambda_o = 45^o$ and diameter of 3 mm. A load cell sensitivity of at least one tenth of that value or 28 gm is required.

Equipment similar to the present apparatus was first used by Bridgman[3] in the same pressure range (0-30 kbar) but differed mainly in the details of the tensile test fixture and in the load cell. Although Bridgman's load cell consisting of a slotted thin tube was the only one reported that could operate in this high pressure range, its inherent sensitivity is not sufficient for the accurate measurement of small loads. Other investigators[4-7] have developed load measuring equipment based on strain gages for use in a high hydrostatic pressure environment with inherent sensitivities greater than that used by Bridgman but it has yet to be shown that these can operate much above the 10 kbar range. The problem associated with strain gage load cells has been the parting of the strain gage from the substrate material due to the stresses arising from the differences in compressibility of the substrate and strain gage materials[8]. Apparatus making use of a load cell the active element of which is a capacitor gage is presently being developed in France[9].

With the possible exception of the equipment incorporating internal load cells based on the capacitance gage principal[9] or cells incorporating alumina coated strain gages[6], all of the thus far developed load measuring equipment associated with mechanical property evaluation at high pressure either is insufficiently sensitive or is limited to ~ 10 kbar.

Equipment

Overall System

The basic pressure generating equipment used was the Birch-Bridgman 30 kbar apparatus[10] manufactured by Harwood Engineering Co. The tensile testing equipment was designed to fit the 3/4 inch diameter bore (1) in the arrangement shown in Figure 1. The tensile load on the sample (2) is produced by the contact of the top piston (3) with the tensile yoke (4) containing the sample and is transmitted through spacer (5) and the load concentrator (6) to the beam of the load cell (7) which is supported on the cylindrical sleeve (8). Electrical connections to the load cell are made through an eight prong radio plug connected to leads which are brought out to the atmosphere through a hardened steel conical pin-lava seal arrangement.

Tensile Yoke

The tensile yoke is similar in concept to that first used by Bridgman[3] and later by others[11-13]. The principal behind its operation is schematically shown in Figure 2 which demonstrates the conversion of a compressive load on the yoke to a tensile load on the sample. A drawing of the actual yoke and sample used in these experiments is shown in Figure 3 and photographs are shown in Figure 4.

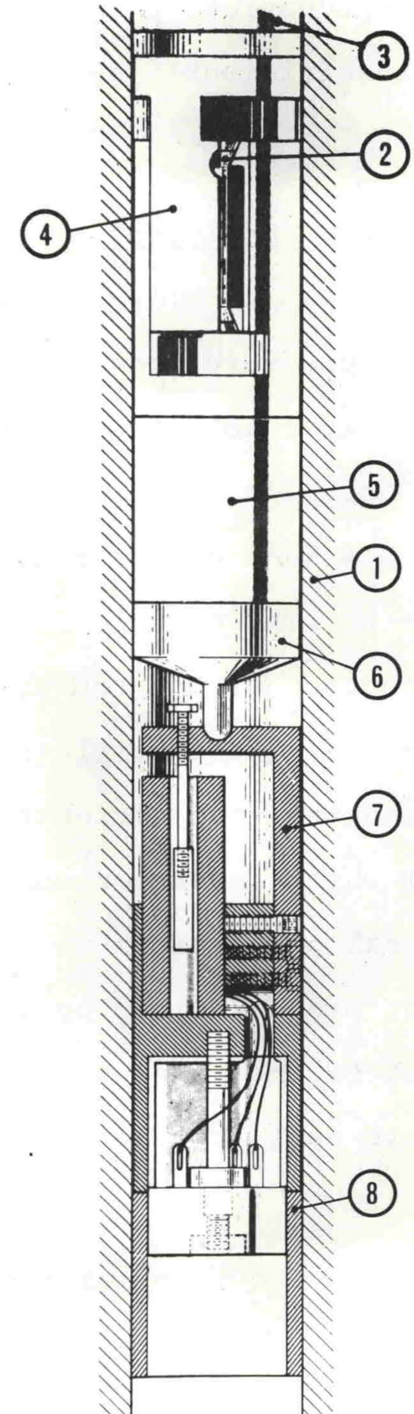

Fig. 1 Schematic representation of high pressure tensile testing apparatus.

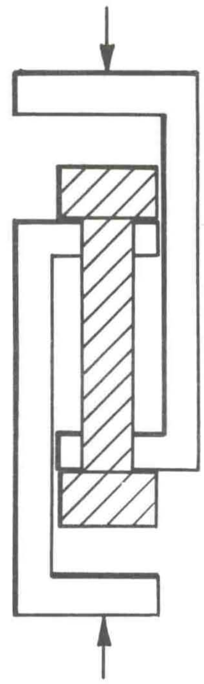

Fig. 2 Schematic representation of principal behind tensile yoke in which an applied compressive load is converted to a tensile load on the sample.

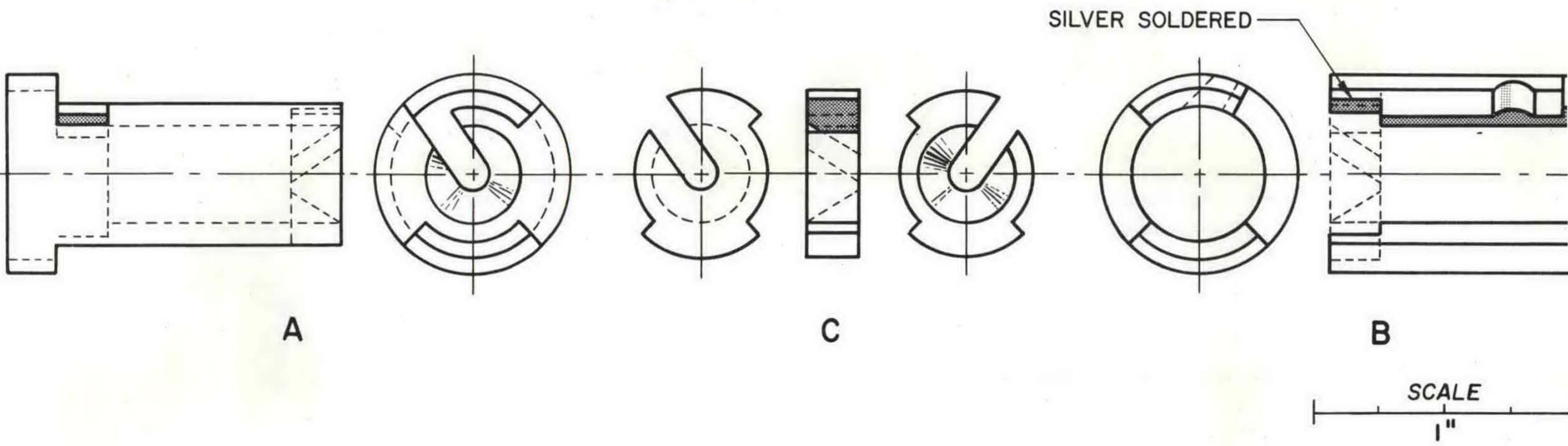

Fig. 3 Diagram of tensile yoke.

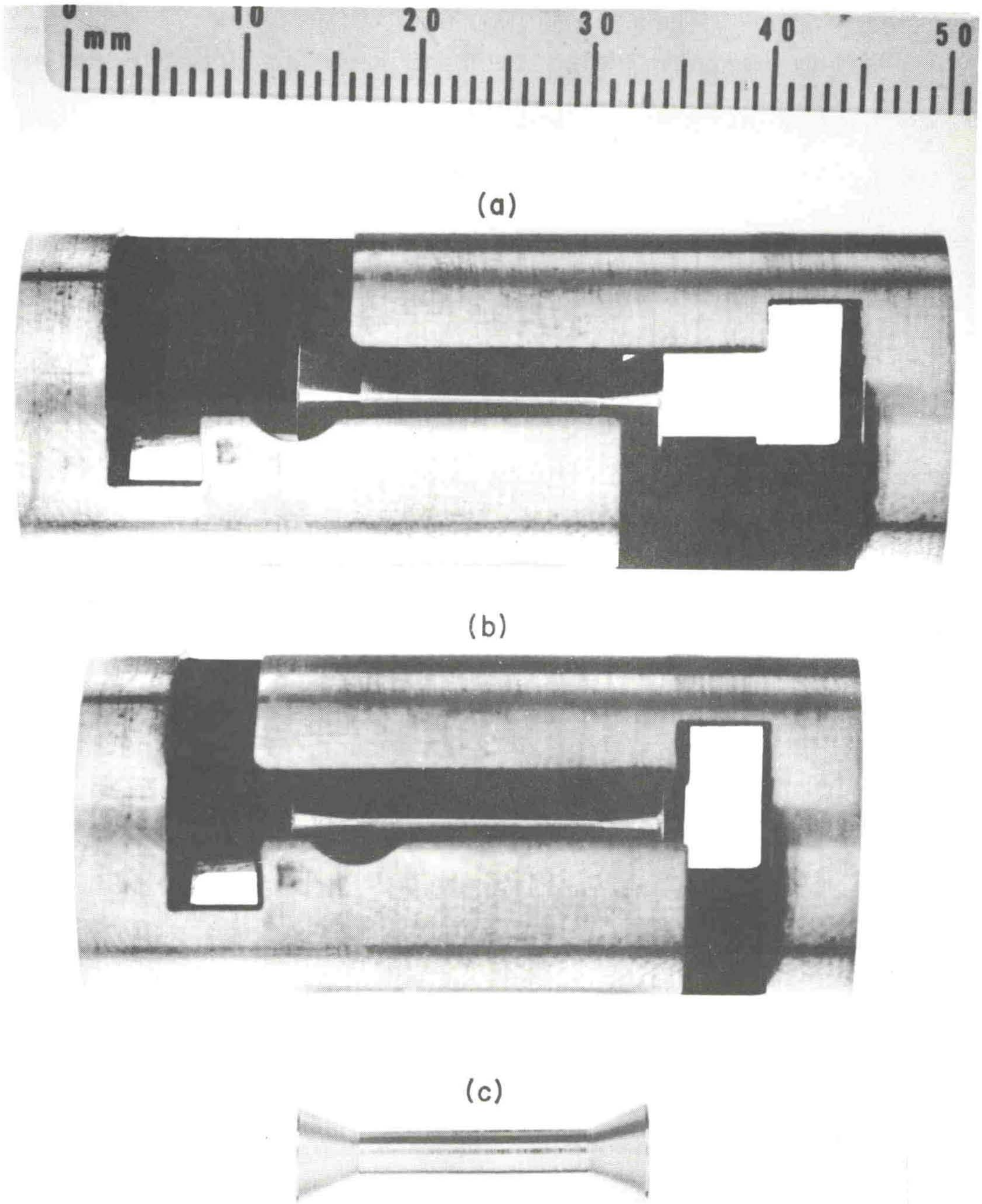

Fig. 4 Tensile yoke in a] position for insertion of sample b] position for testing and c] tensile sample alone.

The sample has an 1/8 inch gage diameter and a 1/2 inch gage length The yoke which is fabricated from high speed steel consists of three pieces A, B and C which are permanently connected by first meshing pieces A and B together and then brazing or soldering piece C in place. As shown in Figure 4, the yoke has been designed so that the sample can be easily dropped into test position through a side slot and an opening enlarged to receive the conical end of the sample. In addition effort has been made to minimize the volume of the yoke so as to provide a maximum volume of the liquid high pressure medium. This in turn will provide a minimum pressure change during sample strain as will be discussed later.

In comparison with other yoke designs this one mainly offers greater ease of assembly and smaller volume. Alignment and frictional effects were the main problem areas. The alleviation of frictional problems in the sliding members and between the yoke and bore of the high pressure unit was accomplished at some sacrifice to alignment perfection but a satisfactory compromise was attained.

<u>Spacer</u>

The tubular spacers (5), Figure 1, which were fabricated from either 2024 aluminum alloy or stainless steel were used to control the pressure at which the mechanical testing was to be performed. This was accomplished by keeping the volume and outside diameter of the spacer constant while changing the spacer height and inside diameter. From the knowledge of the piston position-pressure relationship for a given volume of pressure transmitting fluid, one can predict the pressure at which contact between the upper piston and tensile yoke will occur, i.e. the pressure at the start of the tensile test.

Load Cell

The heart of the apparatus is the load cell. Its operation depends upon the measurement of a beam deflection produced by the applied load through use of a linear variable differential transformer (LVDT).

The load cell which is shown in Figures 5 and 6 is constructed almost entirely of Type 303 stainless-steel. The main body (1) contains a recess for the LVDT (2) and provisions for attaching a beam (3) of the required mechanical sensitivity by means of four stainless steel cap screws (4). Two stainless steel set screws (5) fix the LVDT in position. A partially threaded rod (6) with a hexagonal cross-section head is used to adjust the position of the 50-50 iron-nickel alloy magnetic core (7). A hemispherical recess (8) in the beam allows the load to be concentrated at the center of the beam by means of the load concentrater ((6), Figure 1). The six leads necessary to activate the LVDT and measure its output are connected to a seven prong radio plug (9) which fits into a specially designed bottom connection similar to one previously described[14]. Leads to this connection are brazed to hardened steel conical pins and lead from the chamber as

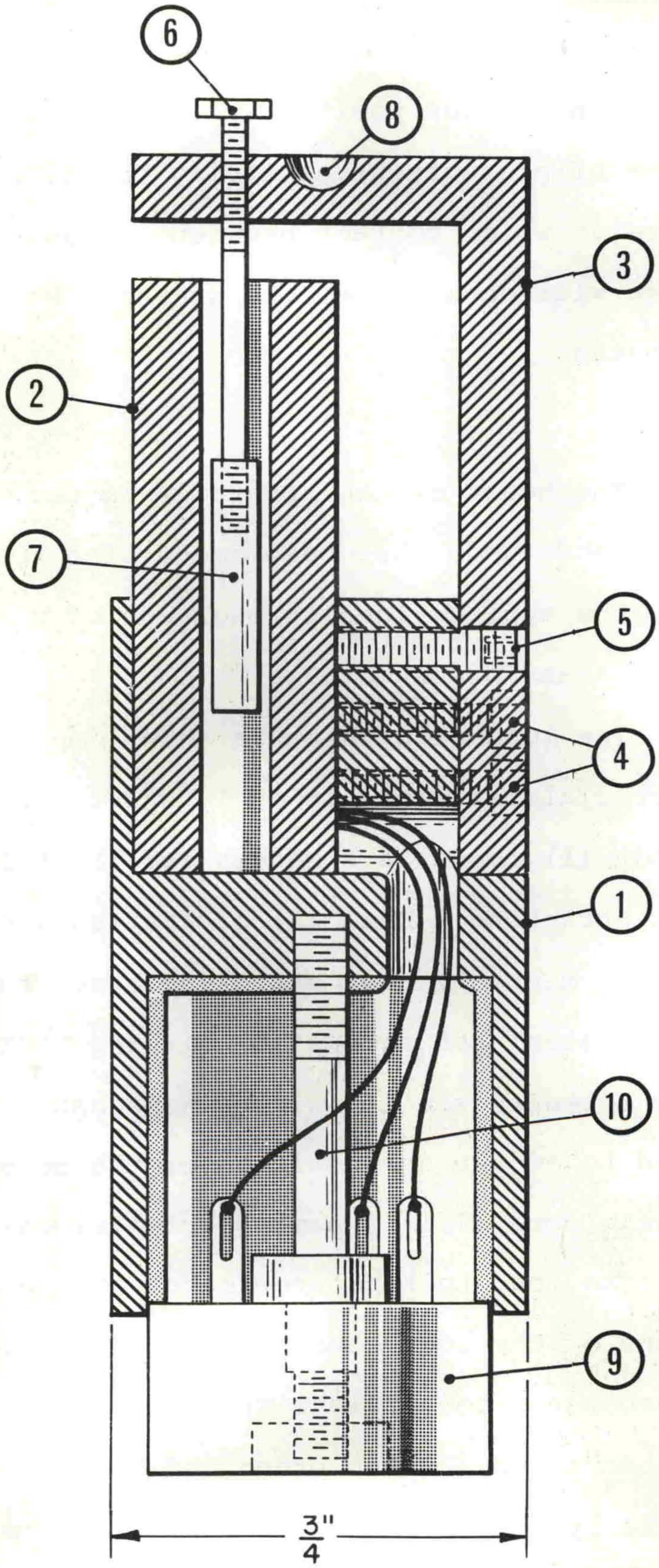

Fig. 5 Sectional drawing of load cell.

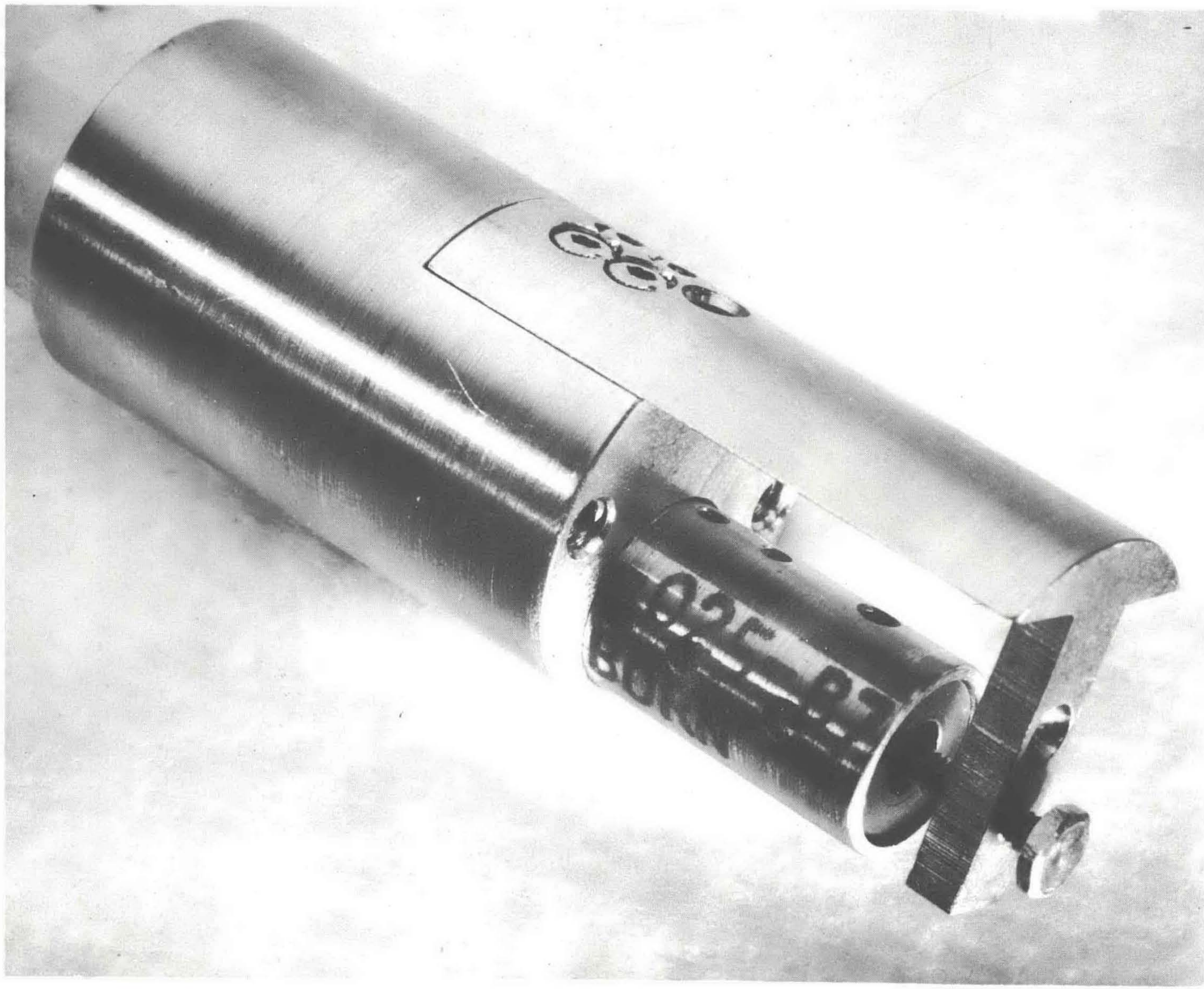

Fig. 6 Load cell 1.4X

previously described. The vertical position of the seven pin radio plug can be adjusted by means of the threaded rod (10) so that good electrical contact can be made and yet have the load cell body bear directly on sleeve (8) Figure 1.

The LVDT which was constructed at the Sanborn Division of Hewlett Packard and Ledgemont Laboratory of Kennecott Copper Corporation is based on a design used in a commercially available LVDT (Sanborn No. 595 DT-025) but with a number of important modifications. Stainless steel was substituted for paper phenolic as the construction materials for the bobbin upon which the transformer coils are wound. A thin (~ 0.005-inch) layer of teflon between the bobbin and magnet wire coils insure electrical insulation. The substitution of stainless steel for the bobbin minimizes coil displacement relative to the core during pressure changes and greatly improves the usable life of the transformer by eliminating coil fatigue failure. This latter effect presumably is caused by the differential expansion and contraction of the phenolic and copper materials owing to their compressability differences. Another difference between the LVDT modified for high pressure use and its commercial cousin is the absence of epoxy potting compounds to maintain the leads and coils in a fixed location. Instead, nylon thread is substituted to tie down the lead wires and coils and to minimize handling stresses on the fine wire coils. The absence of epoxy and the presence of relief holes in the LVDT case maintain an open construction so desirable in high pressure design for the elimination of fluid blockages, unbalanced pressures and resulting large shear stresses.

The LVDT with a linear displacement range of $\sim \pm 0.025$ in. has a sensitivity of ~ 3 volts/inch of core displacement/volt of excitation at a standard carrier frequency of 2400 cycles/sec. Since an excitation voltage of ~ 4.5 volts is supplied by a Sanborn Company Power Supply 850-500-C12, an overall sensitivity of ~ 14 volts/inch of core displacement results. The dimensions of the load cell beam (0.163-in. wide x 0.100-in. high) were chosen to produce a sensitivity of approximately 23 microinch core displacement per pound of applied load. This then provides a load cell output of $\sim 320\ \mu$ V per pound which is amplified with a Sanborn carrier preamplifier 850-1100B. The amplified and phase detected signal is conveniently recorded on one channel of a Moseley X-Y recorder with the preamplifier adjusted to provide 0.1 to 0.5 volts output per pound. The calculated maximum permissable load is 35 lbs, limited by a maximum permitted beam fiber stress of 40,000 psi.

The stiffness of the load cell defined by the displacement of the beam at the position of the applied load (not to be confused with the core displacement) has been calculated to be $\sim 12\ \mu$-in. per pound of applied load.

<u>Strain Measurement</u>

Strain on the sample is measured by monitoring the displacement of the loading piston with a Sanborn LVDT, Model 585DT-500. Although the measurement in fact is not of the sample alone but includes all the components in the loading train, sufficiently accurate measurements of sample length changes are obtained. For instance, sample length changes deduced from piston displacements and corrected for elastic displacements deviated on the average by ± 0.0015 in. from those measured directly on the sample after the test. A large part of this deviation is due to inaccuracies in the measurement of the sample lengths. The instrumentation for this LVDT is similar to that used for the load cell, i.e. Sanborn preamplifier and power supply with the output fed to the second channel of the Moseley X-Y recorder. The LVDT has a sensitivity of ~ 4.5μV/μ-in. of core displacement.

Calibration of the strain measuring LVDT is accomplished by adjusting the preamplifier sensitivity to provide 0.5 V output for 0.010 in. core displacement as deduced from a micrometer drive on the core.

Calibration of the Load Cell

Two methods were used to calibrate the load cell after first establishing that the load-beam deflection relationship was linear. In the first method, the spring constant of an alloy steel helical spring in the form of a tensile sample was measured as a function of pressure and in the second a dead loading method was used.

The spring constant of a helical spring depends upon the shear modulus of the wire from which it is fabricated and its geometry according to the relation:[15]

$$K = \frac{P}{\delta} = \frac{Gd^4}{64nR^3} \qquad (1)$$

where P is the applied load, δ is the spring deflection, G the shear modulus, n is the number of turns, d the diameter of wire and R the radius of the helix. The expected change in spring constant with pressure, α is then:

$$\alpha = \frac{1}{K}\frac{\Delta K}{\Delta P} = \frac{1}{G}\frac{\Delta G}{\Delta P} + \frac{4}{d}\frac{\Delta d}{\Delta P} - \frac{3}{R}\frac{\Delta R}{\Delta P} \qquad (2)$$

Since

$$\frac{1}{d}\frac{\Delta d}{\Delta P} = \frac{1}{R}\frac{\Delta R}{\Delta P} = -\beta \qquad (3)$$

where β is the linear compressibility, the change in spring constant is given by:

$$\alpha = \frac{1\Delta G}{G\Delta P} - \beta \qquad (4)$$

The quantity $\frac{1}{G}\frac{\Delta G}{\Delta P}$ has been measured by Bridgman[16] on hard drawn piano wire and by Birch[17] on drill rod. Their values are 2.19 and 2.4×10^{-6} bar^{-1} respectively. The average, 2.3×10^{-6} per bar, was chosen as a representative value. The value of β is estimated to be 2×10^{-7} bar^{-1} based on Bridgman's measurements[18] of $\Delta V/V_o$ on stainless steel "H29". The value for α is then $\sim 2.1 \times 10^{-6}$ per bar. Deviations from the expected pressure response are due to the change in load cell sensitivity with pressure.

In a typical spring constant calibration experiment, the amplification of the load cell output is adjusted to produce either 0.1 volts per pound or 0.5 volts per pound while dead loading the cell with a 1.5 lb. weight. The load-extension curve is measured at atmospheric pressure and at high hydrostatic pressure (up to ~ 30 kbar). The slope of the curve (see Figure 7) after the initial portion, represents the spring constant. If K_1 represents the spring constant at atmospheric pressure and K^*_P is the measured spring constant at pressure P, C, the correction factor by which measured loads must be divided to obtain true values is given by:

$$C = \frac{\text{Measured Spring Constant at Pressure}}{\text{Theoretical Spring Constant at Pressure}} = \frac{K_P}{K_1(1+\alpha P)} \qquad (5)$$

The best values of C deduced from spring constant calibration experiments are shown in Fig. 8 and are represented by a linear least square fit. It may be seen that as the pressure increases, the load sensitivity decreases. It is estimated that a small part of this decrease is due to an increase of stiffness with pressure of the load cell beam, the remainder of the decrease

---

*It should be noted that the output of the unloaded load cell (zero level) changes somewhat with pressure. This will be discussed later in the paper. The values of K_P have been deduced from the measured slope of the load deflection curve by subtracting the slope of the zero level with deflection. The pressure level also changes somewhat during the spring loading owing to the fact that the pressurizing piston is used to apply the sample load. The spring constant however remains essentially constant in this small pressure interval.

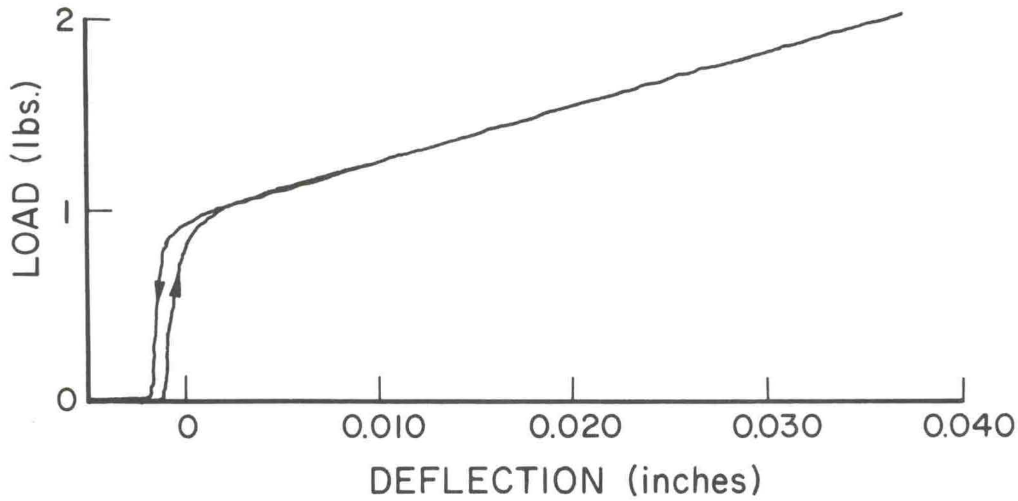

Fig. 7 Load-deflection curve for calibration spring.

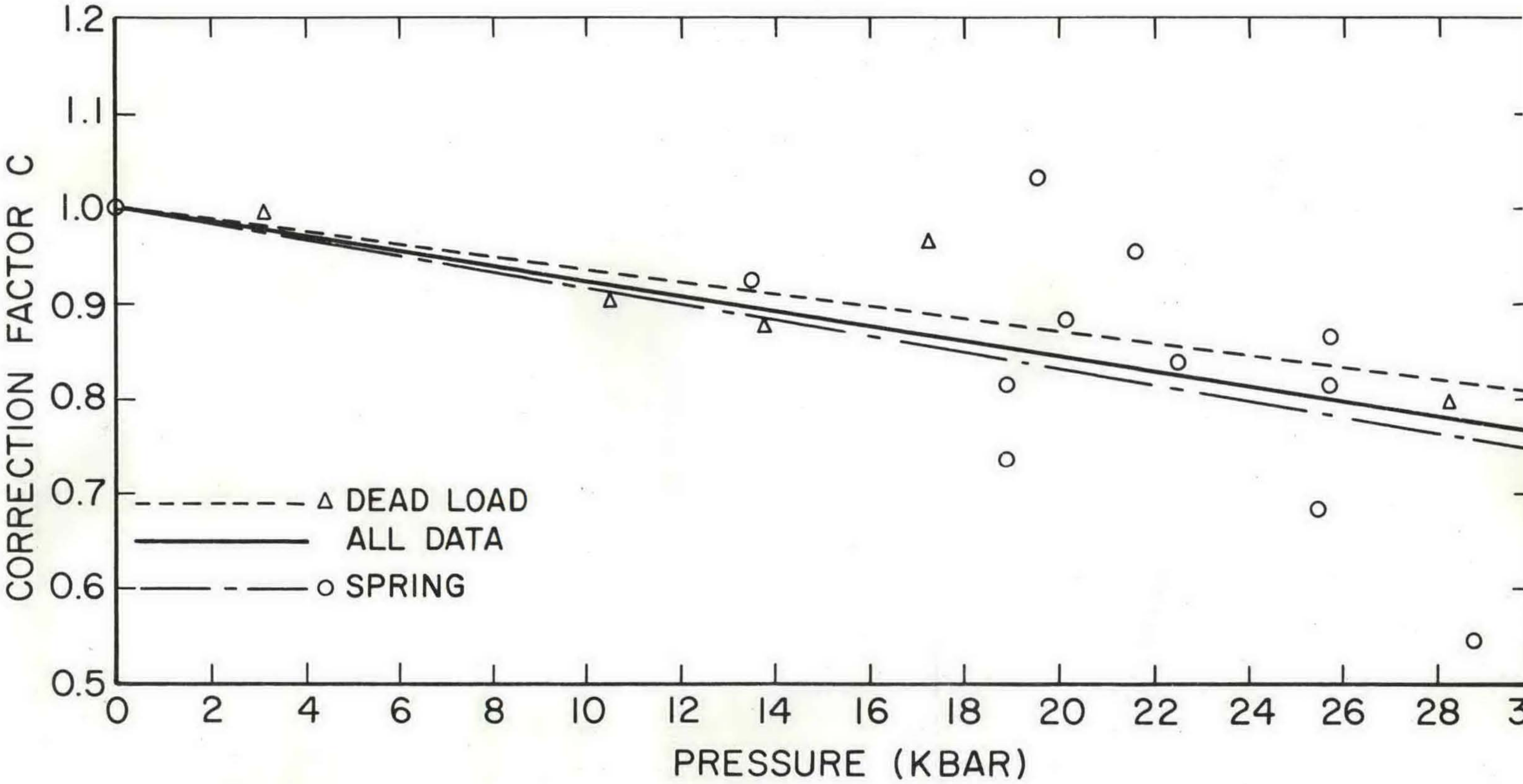

Fig. 8 Pressure variation of load cell sensitivity factor, C.

is presumably due to a change in electromagnetic properties of the core material.

The large amount of scatter in the spring calibration data required us to choose another method of calibration to check the first rather indirect one. The second method was a rather straight forward dead-loading technique. A tungsten weight suspended from the top piston by means of a fine wire (Figure 9) was allowed to contact the spacer above the load concentrator directly (see Figure 1 but with the tensile yoke removed). As the weight contacted the spacer, a conical seat arrangement shown in Figure 9 kept the load constant while the piston continued down for approximately 0.030 in. Thus if load-piston movement is plotted on an X-Y recorder a step function should be seen.

During a dead load calibration experiment, the preliminary adjustment of amplifier sensitivity is carried out in the same manner as in the previous calibration procedure. The load cell is then loaded at atmospheric pressure by use of the conical seat arrangement to ensure that all instrumentation and equipment are functioning normally. Under these conditions, curve of the type schematically shown in Figure 10a is obtained. The system is then pressurized and the response of the load cell to the dead load is measured. The pressure at which the calibration is checked can be adjusted through proper choice of the spacer located above the load concentrator. Curves obtained under pressure are similar to that shown schematically in Fig. 10b. The vertical displacement, Y_p, is taken as the measured load at high

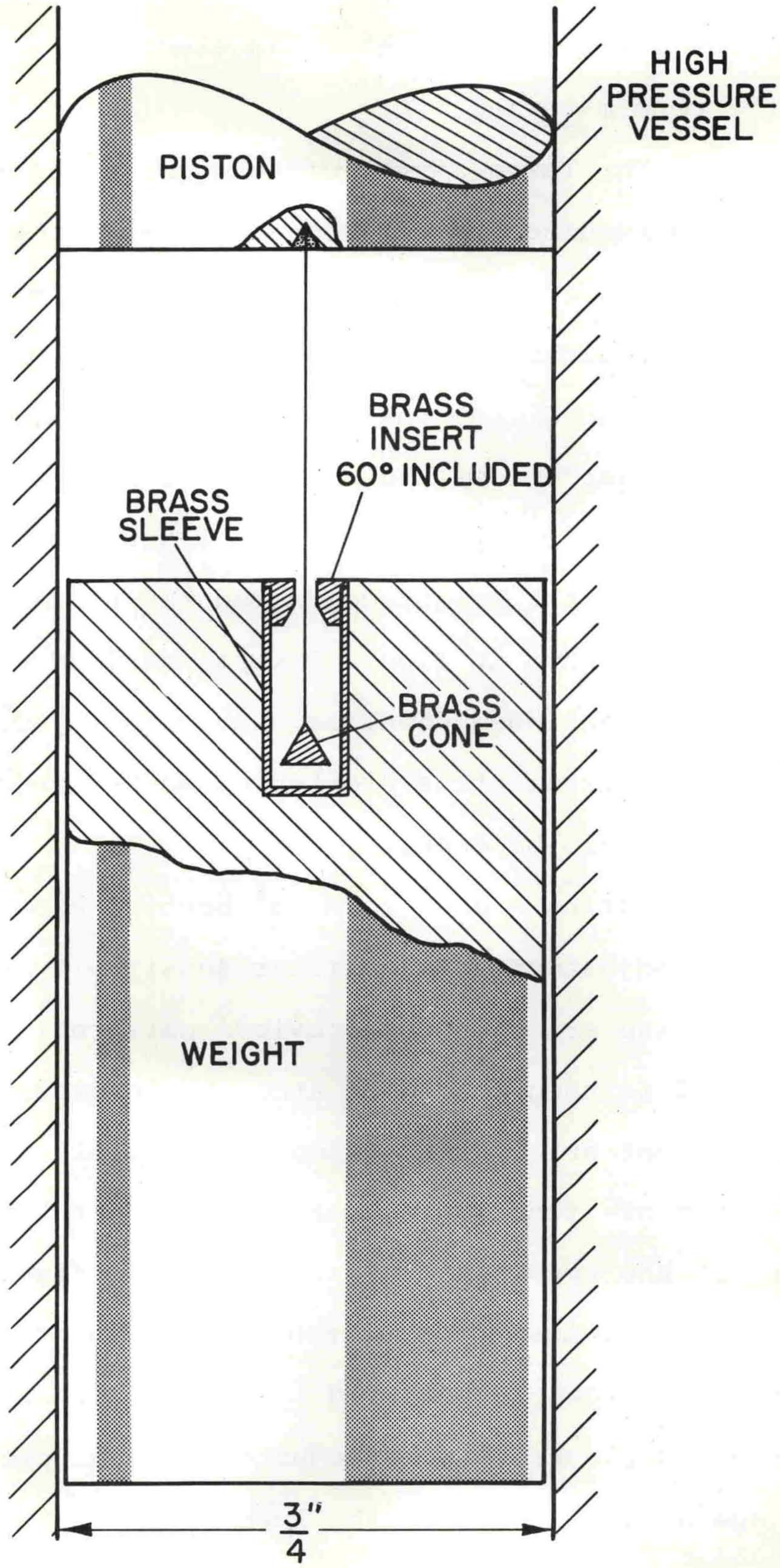

Fig. 9 Dead load calibration apparatus.

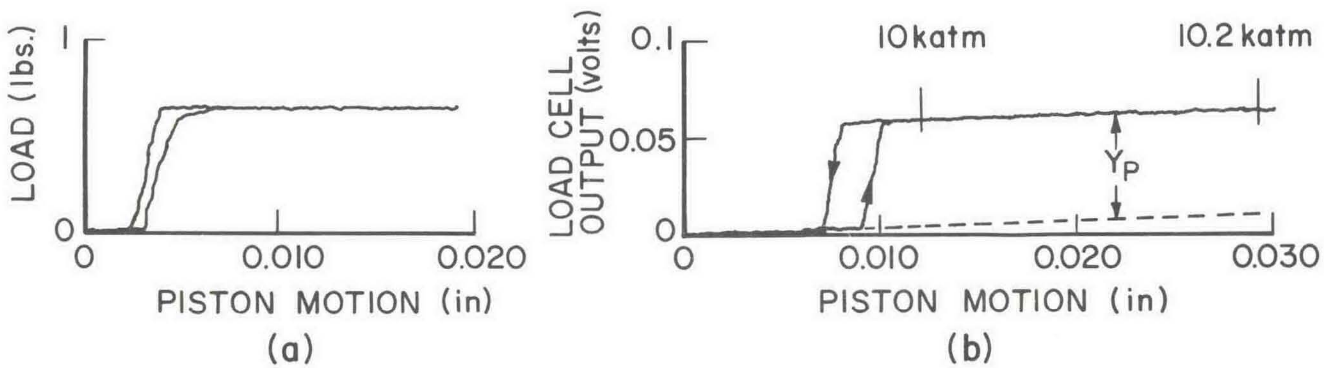

Fig. 10 Dead load calibration plots a] test at atmospheric pressure b] test at high pressure.

pressure. This value includes the change in sensitivity of the load cell with pressure, the change in buoyancy of the pressure medium and as shown is corrected for the change in zero load level with pressure. In order to calculate the correction factor, C, it was necessary to deduce the buoyant force from the volume of the tungsten weight and the variation of the density of high pressure medium with pressure, $\rho(P)$. $\rho(P)$ can be deduced from ρ_o, the density at atmospheric pressure[19] and the variation of V_P/V_o with pressure by the relation:

$$\rho(P) = \frac{\rho_o \, V_o}{V_P} \tag{6}$$

V_P is the volume of liquid at pressure, P, and V_o is the volume of liquid at atmospheric pressure.

As shown in Fig. (11), V_P/V_o is known as a function of pressure from another experiment[20] for a 50 volume percent mixture of n- and i- pentane. The correction factor C is then equal to the recorded load at pressure divided by the true load at pressure or

$$C = \frac{Y_P}{Y_o - V_w \rho_P} \tag{7}$$

where Y_o is the weight of the tungsten dead load in air at atmospheric pressure, V_w is the volume of the tungsten weight and ρ_P is the density of the medium at pressure.

A number of dead load calibration experiments have been performed with the results shown in Figure 8. The linear

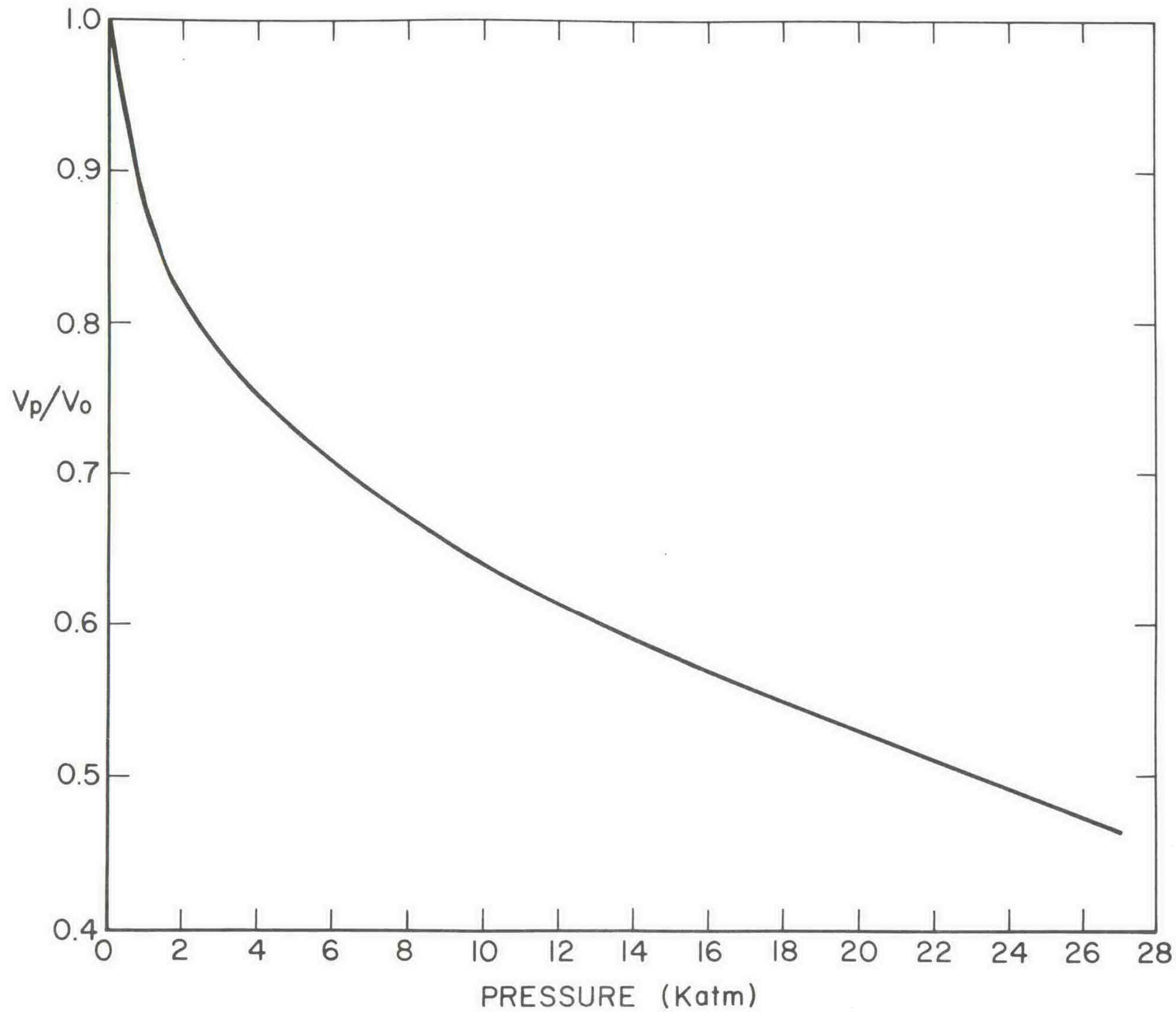

Fig. 11 V_P/V_o as a function of pressure. 50-50 volume percent mixture of i- and n- pentane - 22°C.

least square fit for this data is shown as the dashed line in this figure. The individual data points show considerably less scatter than the spring calibration data.

In both the case of the spring constant calibration and dead load calibration, linear list square fits are given for weighted data. The weighting factor was based upon the scatter found on repeated loading in a given experiment. The data point, C = 1 at atmospheric pressure was given a weighting factor of 5. Weighting factors for the other data points ranged between 1 and 5.

As may be seen from Figure 8 the agreement between the linear representations of the correction factor - pressure relationships deduced from the spring constant and dead load calibrations is quite good.

Also included in Figure 8 is the weighted linear least square fit for the combined data of the spring and dead load calibrations. From this latter data $C = 1 - 9.1 \times 10^{-3}P$ for P expressed in kbar.

Test Procedure

Before a typical tensile test is performed, the load cell and strain measuring LVDT are balanced and the calibrations are checked by dead loading the load cell with a known weight and displacing the core of the strain measuring LVDT by a known amount. A number of atmospheric pressure tests are then conducted using the steel spring tensile sample. This procedure insures that alignment in the apparatus is good and that friction either in the sliding parts of the tensile yoke or between the yoke and pressure vessel walls is not excessive. The steel spring sample is then replaced by the tensile sample of interest, and the tensile yoke and sample are inserted in the high pressure vessel atop of the cylindrical spacer in the arrangement of Figure 1. The spacer is chosen so that contact between the pressurizing piston and tensile yoke will occur at a predetermined pressure. The distance between the top of the pressure vessel and the tensile yoke is then accurately measured with a depth gage, the system filled with fluid and the top seal inserted. The system is then pressurized by driving the top piston downward to within approximately 0.100 inch of the tensile yoke as measured by a dial gage attached to the piston on the pressurizing jack. During pressurization the output of the load cell is recorded as a function of pressure and time. The strain measuring LVDT is then set so that the core position is within the linear range of the transducer and the pressurization is continued by hand pumping while recording the output of the load cell and strain measuring LVDT on an X-Y recorder. At contact between piston and tensile yoke there is a discontinuity in the load cell output marking the start of the recording of sample load vs. extension. A typical load-extension curve of a zinc single crystal tested at high pressure is shown in Figure 12.

A number of features of this curve are noteworthy. First of all there is a small change in pressure during the

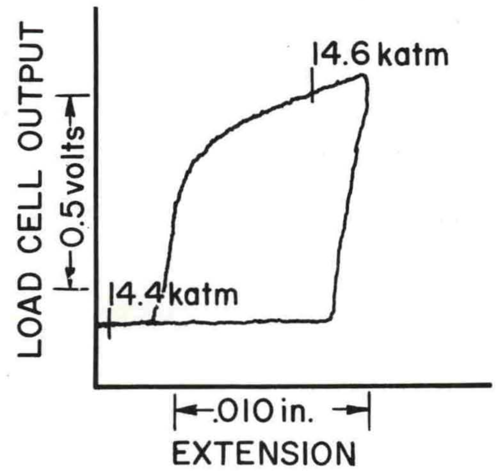

Fig. 12 Load-extension curve for zinc single crystal stretched at a pressure of ~ 14.5 katm.

tensile test since the piston which produces the load on the sample also pressurizes the system. This is a minor inconvenience in our experiments since the small strains to which the samples were subjected (~0.010 inch piston motion) produced very small pressure changes. Another feature which should be pointed out is the change of load cell output voltage (zero load level) with pressure. This variation is represented in Figure 13 where it may be seen that the rate of voltage change with pressure decreases with increasing pressure. The output voltage-pressure relationship was of approximately the same form from experiment to experiment. However, a hysteresis effect has been noted. This is characterized by a smaller zero level output voltage for a given pressure after the load cell had been subjected to the highest pressures (30 k atm.). The output-voltage for a given pressure gradually increases with subsequent experiments at moderate pressures. A similar type of behavior was also noted during the calibration experiments where on repeated loading in a given pressure range the variation with pressure of the zero level decreased markedly after the initial loading. The effect of pressure on the zero output level is accounted for by subtracting its variation with piston position from the output voltage-piston position curve representing the tensile test.

Discussion

Although the apparatus provides the required com-

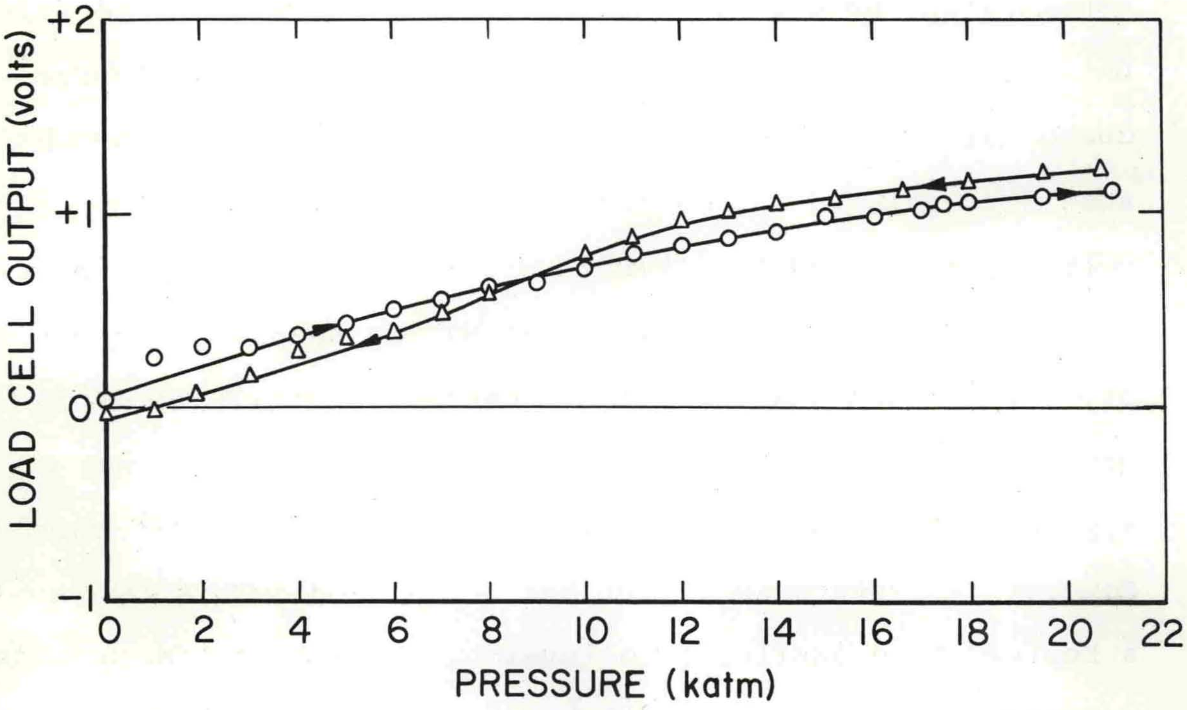

Fig. 13 Load cell output vs. pressure for unloaded cell (zero level).

bination of high sensitivity and high pressure capability it is still not without operational difficulties. The variation of load cell zero out-put level with pressure is one already described in detail. Its form, showing large variation at low pressure and smaller variation at high pressure suggests that the effect may be due to small differences in the linear compressibility of the load cell construction materials. Hysteresis effects which may be related to those observed in the load cell behavior have also been encountered in the compression of similar material[18].

The change in load cell sensitivity with pressure is also of importance. The reason for this variation is not understood but is probably caused by changes in the electrical and magnetic properties of the core alloy, Fe -50 pct Ni; changes in magnetic permeability of this alloy with pressure have been reported[21]. Choice of other materials for the core could probably eliminate the sensitivity change with pressure.

The above difficulties are minor inconveniences which have been resolved by computer corrections to load-extension data. Only little additional effort was required since load-extension curves were already being converted with computer aid to shear stress-shear strain curves, resolved along the glide plane in the glide direction.

Another potential problem which may be encountered is due to frictional effects. Friction between the sliding members of the tensile yoke and between the yoke and inner walls of the chamber may give rise to innaccurate load-extension curves. Such frictional effects often arise from innaccurate alignment or oxide or dirt on the sliding surfaces and they may be eliminated by correcting these difficiences. The absence of gross frictional effects can be confirmed by comparing the 1 atm. load-extension curves of the spring tensile sample during loading and unloading. If frictional effects are absent these curves should be identical. Unfortunately there is no easy check for friction at high pressure since the values of displacement on unloading are innaccurate.

The heart of the apparatus, the load cell, can of course be used in measuring loads in other types of mechanical tests such as compression, bending or hardness. The sensing element in this device, the LVDT modified for high pressure operation also lends itself for use in equipment in which linear motion is to be measured at high pressure. Such measurements include compressibility,thermal expansion, dilatometry etc.

Summary

Apparatus has been described which allows the tensile testing of soft materials at pressures which are currently limited by the solidification of the pressure medium, ~ 30 kbar. The apparatus makes use of a convenient tensile yoke and a load cell having an LVDT modified for high pressure operation as a sensing element. The effect of pressure on the operation of this equipment has been discussed.

Acknowledgement

The author greatly appreciates the aid of Carl Bomhard and Eric Stroberg of Ledgemont Laboratory in the construction and design of the tensile yoke and load cell. Special thanks are also due T. Garber and S. Sycorcua of Sanborn Division of Hewlett Packard Co. for their help in the design of the LVDT modified for high pressure. The author especially appreciates the aid of Peter Femino of Ledgemont Laboratory in the conducting and evaluation of the experimental tests of the equipment.

Footnotes

1. P. W. Bridgman, The Physics of High Pressure (G. Bell and Sons Ltd., London, 1958) p 399.
2. S. H. Gelles, Accepted for publication, J. Chem. Phys.
3. P. W. Bridgman, Studies in Large Plastic Flow and Fracture (Harvard University Press, Cambridge 1964).
4. P. Haasen and A. W. Lawson, Jr., Z. Metallk. 49, 280 (1958).
5. J. E. Hanafee and S. V. Radcliffe, Rev. Sci. Instr. 38, 328 (1967).
6. Robert B. Gordon and Leslie F. Mike, Rev. Sci. Instr. 38, 541 (1967).
7. H. Ll. D. Pugh, Irreversible Effects of High Pressure and Temperature on Materials (American Society for Testing and Materials, Philadelphia, 1956) p 81.
8. R. V. Milligan, Experimental Mechanics 4, 25 (1964).
9. D. Francois, CEA France, Personal Communication.
10. F. Birch, E. C. Robertson and S. P. Clark, Jr., Ind. Eng. Chem. 49, 1965 (1957).
11. B. I. Beresnev et al., Some Problems of Large Plastic Deformation of Metals at High Pressure (The Macmillan Co., London 1963) p 15.
12. E. A. Stack and A. Bobrowsky, Beryllium Technology (Gordon and Breach, Science Publishers, New York 1966) p 411.
13. M. Brandes and H. Szlacheic, Rev. Sci. Instr. 36, 991 (1965).
14. T. E. Davidson and A. P. Lee, Trans. AIME, 230, 1035 (1964).

15. S. Timoshenko, Strength of Materials, Part I (D. Van Nostrand Co., New York, 1962) p 293.

16. P. W. Bridgman, Proc. Am. Acad. Arts. Sci. 63, 401 (1929).

17. Francis Birch, J. Appl. Phys. 8, 129 (1937).

18. P. W. Bridgman, Proc. Am. Acad. Arts Sci. 77, 189 (1949).

19. International Critical Tables, Vol. III (McGraw Hill Book Co., New York, 1928).

20. S. H. Gelles, Unpublished data.

21. D. Gugan, Proc. Phys. Soc. (London) 72, 1013 (1958).

DISTRIBUTION LIST TR-164

Internal

E. W. Fletcher

C. G. Lindquist

D. A. Corrigan

P. J. Femino

W. W. Harvey

W. H. L. Hooper

D. H. Howling

E. D. Levine

I. S. Servi

C. C. Wang

LEDGEMONT LABORATORY

KENNECOTT COPPER CORPORATION

LEXINGTON, MASSACHUSETTS

Technical Number: TR-164 Dated: 26 Feb. 1968

Title and Author

Apparatus for Mechanical Testing of Soft Crystals at High Pressure

S. H. Gelles

Publisher: Submitted to: Rev. Sci. Instr.

Pages: 30

Illus. 13

Abstract: Apparatus which has sufficient sensitivity for the tensile testing of soft single crystals at pressure levels to approximately 30 kbars is described. This equipment makes use of a tensile yoke and a load cell based on a linear variable differential transformer within the high pressure fluid. Strain is measured externally by monitoring the movement of the loading piston with a linear variable differential transformer and the load-displacement relationship is displayed on an X-Y recorder. Discussion of the calibration procedure and performance of the apparatus is included.